The interaction between the spin transition and a crystallographic phase transition in the spin-crossover compound [Fe(bbtr)3](ClO4)2: Nucleation, formation of domains and fluctuations

Krivokapic, Itana; Enachescu, Cristian; Bronisz, R.; Hauser, Andreas

How to cite

KRIVOKAPIC, Itana et al. The interaction between the spin transition and a crystallographic phase transition in the spin-crossover compound [Fe(bbtr)3](ClO4)2: Nucleation, formation of domains and fluctuations. In: Inorganica Chimica Acta, 2008, vol. 361, n° 12-13, p. 3616–3622. doi: 10.1016/j.ica.2008.03.064

This publication URL: https://archive-ouverte.unige.ch/unige:3576

Publication DOI: 10.1016/j.ica.2008.03.064

Inorganica Chimica Acta 361 (2008) 3616–3622

Contents lists available at ScienceDirect

Inorganica Chimica Acta

journal homepage: www.elsevier.com/locate/ica

The interaction between the spin transition and a crystallographic phase transition in the spin-crossover compound $[Fe(bbtr)_3](ClO_4)_2$: Nucleation, formation of domains and fluctuations

Itana Krivokapic [a], Cristian Enachescu [b,*], Robert Bronisz [c], Andreas Hauser [a,*]

[a] Département de chimie physique, Université de Genève, 30, quai Ernest-Ansermet, 1211 Genève 4, Switzerland
[b] Department of Physics, Al. I. Cuza University, 700506 Iasi, Romania
[c] Faculty of Chemistry, University of Wroclaw, F. Joliot-Curie 14, 50-383 Wroclaw, Poland

ARTICLE INFO

Article history:
Received 28 February 2008
Received in revised form 6 March 2008
Accepted 10 March 2008
Available online 19 March 2008

Dedicated to Dante Gatteschi in honour of his contribution in the field of molecular magnetism.

Keywords:
Iron(II) spin-crossover complex
High-spin → low-spin relaxation
Crystallographic phase transition
Light-induced spin transition

ABSTRACT

The thermal and the light-induced spin transition in $[Fe(bbtr)_3](ClO_4)_2$ (bbtr = 1,4-di(1,2,3-triazol-1-yl)) as well as the high-spin → low-spin relaxation following the light-induced population of the high-spin state below the thermal transition temperature are discussed in relation to the accompanying crystallographic phase transition. The experimental data have exclusively been obtained using optical single crystal absorption spectroscopy.

1. Introduction

Spin-crossover compounds [1] are compounds of octahedral complexes of transition metal ions having d^4 to d^7 electron configurations. They are among the few systems showing bistability at a molecular scale with switchable properties induced by variations of temperature [2,3], pressure [4,5] or by light-irradiation [6]. This makes them interesting for potential application such as high-density information storage systems [7] and displays [8]. By far the largest number of known spin-crossover systems have d^6 iron(II) as central ion, for which the transition occurs between the low-spin (LS) $^1A_1(t_{2g}^6)$ state and the high-spin (HS) $^5T_2(t_{2g}^4e_g^2)$ state. The thermal transition is entropy driven by both the electronic degeneracy of the HS state as well as the vibrational contribution, and it always occurs from the diamagnetic LS state populated at low temperatures to the paramagnetic HS state populated at elevated temperatures. Due to elastic interactions between the spin-crossover units resulting from the large difference in metal–ligand lengths between the two spin states, the thermal spin transition is very often much more abrupt than predicted by a simple Boltzmann distribution between the two vibronic manifolds. If the elastic interactions between the spin-crossover units are large enough, it may even occur as a first order transition and show a thermal hysteresis [2,3]. Such cooperative effects have been and continue to be of interest, as they constitute an essential ingredient for the macroscopic bistability and memory effects needed for the above-mentioned potential applications. Of particular interest, in the context of the work presented in this paper, are systems in which the spin transition triggers a crystallographic phase transitions as for instance in the model compound $[Fe(ptz)_6](BF_4)_2$ (ptz = 1-propyltetrazole) [9–12], or induces a super-structure such as in $[Fe(pic)_3]Cl_2 \cdot EtOH$ [13,14], and may even lead to a self-grinding effect reducing the crystallite size to a comparatively homogeneous distribution of the order of micrometres [15].

At low temperatures iron(II) spin-crossover systems can be switched from the ground LS state to the long lifetime metastable HS state by using light of appropriate wavelengths, a phenomenon known as Light-Induced Excited Spin State Trapping (LIESST) [2,16]. The at low temperatures metastable HS state relaxes towards the ground state by a non-adiabatic, non-radiative process [17], that is by a slow tunnelling process below ~50 K and thermal activation above that temperature. Cooperative effects also influence the kinet-

* Corresponding authors.
E-mail addresses: cristian.enachescu@uaic.ro (C. Enachescu), andreas.hauser@chiphy.unige.ch (A. Hauser).

0020-1693/$ - see front matter © 2008 Elsevier B.V. All rights reserved.
doi:10.1016/j.ica.2008.03.064

ics of the relaxation process, resulting in highly non-exponential relaxation curves [18]. In some compounds, a reverse photophysical process with irradiation at 830 nm known as reverse-LIESST can also reconvert the light-induced HS state back to the ground state [6].

The most simple model treats the cooperative effects in a mean-field approach [19,20]. This model was successfully applied to a number of systems with moderate interaction parameters [18,21,22], but its performance was less satisfactory for strongly cooperative systems showing hysteresis behaviour. Some 18 years ago, Sorai et al. [23] suggested that in such systems the spin transition occurs through domains of like spins, that is, through the formation of domains consisting of molecules of the same spin state. Over the past few years, the existence of such like spin domains was inferred from experimental data, namely the observation of minor hysteresis loops for thermal and light-induced thermal transitions [24,25], X-ray diffraction data [26], Raman scattering during the thermal transition [27], and neutron Laue scattering on single crystals [28]. Several models derived mainly from the analysis of domains in magnetic systems such as Preisach type models [24] or the First Order Reversal Curves (FORC) method [29–31] revealed that in the case of powder samples the domains may be regarded as independent.

In the present paper we discuss the formation and existence of like spin domains in single crystals of $[Fe(bbtr)_3](ClO_4)_2$ (bbtr = 1,4-di(1,2,3-triazol-1-yl)) during the thermal spin transition as well as during relaxation following irradiation. This compound presents a 2D polymeric type structure with every Fe^{2+} centre surrounded by six ligands and every ligand acting as bridging ligand between two Fe^{2+} centres. This results in a high degree of cooperativity, which manifests itself in a thermal spin transition with a 15 K wide hysteresis centred around 105 K. The system presents two crystallographic phases: an ordered phase at above the spin transition temperature having space group $P\bar{3}$, and a disordered phase below the spin transition temperature for which to date it has not been possible to determine the crystal structure [32]. The crystallographic phase transition from ordered to disordered phase has been associated with a nucleation and growth process and domain formation in a previous communication [33]. In order to clarify the complex behaviour of this system, we provide in this paper a full analysis of its thermal spin transition, low temperature photoexcitation and finally of the relaxation curves inside the thermal hysteresis.

2. Experimental

See the paper by Bronisz [32] for a detailed account of the synthesis, crystal growth and high-temperature crystal structure determination of the title compound. The high-quality $[Fe(bbtr)_3](ClO_4)_2$ crystals of $\sim 0.4 \times 0.4 \times 0.2$ mm^3 used in the present study were likewise grown by Bronisz. They are hexagonal with well-developed faces, transparent at room temperature and red at cryogenic temperatures. They cleave easily perpendicular to the *c*-axis. The experimental data presented in this paper were exclusively obtained from optical absorption measurements on single crystals. For these measurements, crystals cleaved to approximately 60 μm thickness were mounted on a small aperture in a copper sample holder using silver contact glue. For temperature dependant measurements between cryogenic and room temperature, the sample holder was inserted into a closed cycle cryostat capable of achieving temperatures down to 4 K (Janis Research) and equipped with a programmable temperature controller allowing variable temperature scans. For irradiation experiments involving LIESST and reverse-LIESST at temperatures below 20 K, the light of a continuous Ar/Kr mixed gas laser at 488 nm (Spectra Physics 2018) or of a Xe-arc lamp and a laser diode at 830 nm (ILEE Model Z40KV1) were used, respectively. With laser powers of ~6 mW/mm^2 a quantitative population of the HS state was achieved in <30 s. High-quality absorption spectra between 9000 and 28 000 cm^{-1} (400–900 nm) were recorded on a Fourier transform spectrometer (Bruker IFS66) equipped with the respective beam splitters and detectors. Kinetic experiments at fixed temperatures and temperature scan experiments were performed on a home-built system consisting of a 0.28 m monochomator (Spex 280M, holographic grating with 150 grooves/mm) equipped with a CCD camera (Jobin-Yvon Spex CCD 3500) and polychromatic light from a 50 W tungsten halogen lamp as probe beam. This set-up allowed recording a full spectrum between 10 000 and 25 000 cm^{-1} at given time intervals, the minimum time interval between two spectra being 3 s. In order to minimize the amount of light from the 50 W tungsten halogen lamp falling on the sample, neutral density filters were used to attenuate the light to <2% of its full intensity and the probe beam was gated with a shutter in parallel to the shutter of the CCD camera. Thus the effects of the probe beam are negligible with regard to the light-induced spin transition. For the HS → LS relaxation experiments at a fixed temperature, the initial population of the HS was achieved below 20 K using comparatively high laser powers of 20 mW/mm^2, then the temperature was raised to the target temperature within <2 min. The laser was kept on the sample until this temperature was reached, and switched off as the relaxation experiment was started. This procedure ensured that even for relaxation curves at comparatively high-temperatures, that is, approaching the thermal transition temperature, the initial HS population was close to 100%. For additional irradiation experiments inside the thermal hysteresis, a frequency doubled pulsed Nd:YAG laser (Quantel Brilliant B) was used.

For both the temperature dependent absorption spectra as well as the time dependent spectra, the fraction of complexes in the HS state can be extracted from the relative intensities of the typical absorption bands of the HS and the LS species [34]. By recording full spectra, artefacts due to baseline shifts from variations in diffuse scattering can be eliminated. For the analysis of the temperature dependent spectra, the small temperature dependence of the oscillator strength of the respective transition was neglected.

3. Results and discussion

3.1. Absorption spectra during the thermal spin transition

Fig. 1 shows the high-quality single crystal absorption spectra of $[Fe(bbtr)_3](ClO_4)_2$ with the light propagating along the *c*-axis (α spectrum) at 295 K and at 10 K on slow cooling. At room temperature, when all complexes are in the HS state, the spectrum shows the typical near infrared band of the HS species centred at 12 000 cm^{-1} (833 nm) corresponding to the $^5T_2 \rightarrow {}^5E$ ligand-field transition. The 10 K spectrum is characteristic for the LS species with the more intense absorption band in the visible centred at 18 000 cm^{-1} (590 nm) and corresponding to the $^1A_1 \rightarrow {}^1T_1$ ligand-field transition. In accordance with magnetic susceptibility measurements on a polycrystalline sample [32] the thermal spin transition is complete with neither a residual HS fraction at low temperature nor a residual LS fraction at high-temperature.

With temperature quenching, that is, very fast cooling at >60 K/min starting from room temperature down to <60 K, the complexes can be trapped almost quantitatively in the HS state. Fig. 1 includes the absorption spectrum of the title compound at 10 K in this trapped HS state, with a LS fraction of only ~10%. At 10 K the temperature quenched HS state has a very long lifetime. This is discussed in more detail in Section 3.4.

Fig. 2 shows the absorption spectrum of the title compound as a function of decreasing temperature between 110 and 90 K at a cooling rate of 0.03 K/min on starting from room temperature.

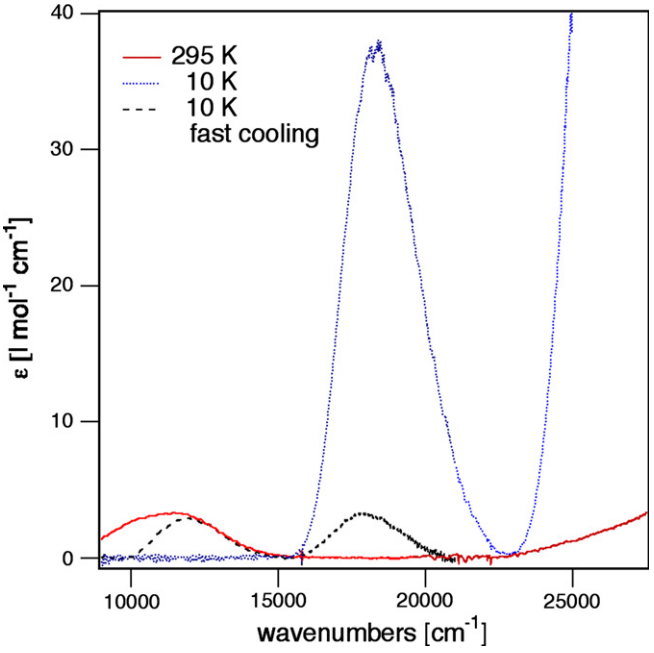

Fig. 1. Single crystal absorption spectrum of $[Fe(bbtr)_3](ClO_4)_2$ at 295 K (—) and at 10 K on slow cooling (. . .) and after temperature quenching (- - -).

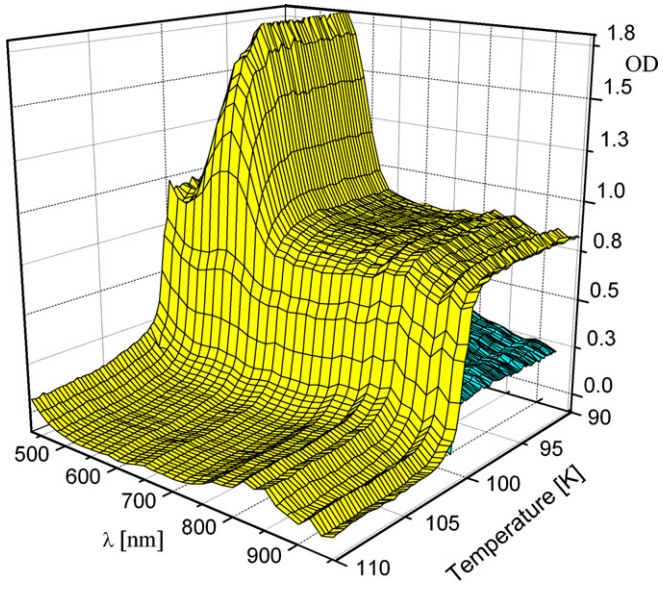

Fig. 2. Single crystal absorption spectrum of $[Fe(bbtr)_3](ClO_4)_2$ (d = 60 μm) during the thermal transition on cooling with a rate of 0.03 K/min from room temperature (top sheet) and from 120 K on the second cycle (bottom sheet).

While decreasing the temperature, the HS band in the near infrared disappears abruptly at around 100 K and is replaced by the more intense LS band in the visible, indicating that the thermal HS → LS transition occurs at $T_c^{\downarrow} \approx 100$ K. Concomitantly with the spin transition a marked baseline shift in the optical spectrum is observed. This is due to an increase in wavelength independent diffuse scattering, and indicates that at the spin transition temperature domains with a domain size of the order of the wavelength of light develop. This effect occurs right at the beginning of the transition when the LS fraction is still low, indicative of a nucleation and growth process. On heating the crystal to 120 K, that is, above the thermal LS → HS transition at $T_c^{\uparrow} \approx 113$ K [32], and subsequent cooling down at the same rate, the thermal HS → LS transition occurs at distinctly higher temperature than on the first cooling down. This is to be discussed in some detail in Section 3.3. The point to note here is that the accompanying baseline shift is much smaller than on the first cooling cycle. Thus even though at 120 K a HS fraction of 1 is restored, the system keeps a memory of the domain structure resulting form the first cooling cycle. This domain structure is only annealed upon heating the sample to above 200 K.

3.2. LIESST, reverse-LIESST and the HS → LS relaxation at low temperature

As mentioned in the introduction, many spin-crossover systems, especially those with triazole and tetrazole ligands exhibit the phenomenon of LIESST. Fig. 3 shows the absorption spectrum of the title compound at 10 K before and after irradiation with a broad band Xenon arc lamp. Irradiation completely bleaches the characteristic LS absorption bands indicating a quantitative LS → HS transformation. At 10 K the system remains trapped in this metastable HS state for a very long time because of the large energy barrier between the two states resulting from the large bond length difference and at the same time small energy difference. At temperatures >50 K, relaxation back to the LS ground state sets in (see below). The system can also be reconverted to the LS state at 10 K by irradiating at 830 nm, that is, into the near-infrared band of the HS species. Fig. 3 includes the corresponding absorption spectrum after prolonged irradiation at 830 nm (2 mW/mm^2) showing that in reverse-LIESST a saturation value of the LS fraction of 85% is obtained [6].

Quantitative photoexcitation experiments were performed at 10 K using the 488 nm line of an Ar–Kr cw laser. Fig. 4 shows photoexcitation curves obtained from recording full absorption spectra at given time intervals for three different light intensities. The time necessary to populate the HS state quantitatively is 30 s for a laser power of ~6 mW/mm^2 at the sample. With a laser power of 0.02 mW/mm^2 a quantitative population of the HS state can still be achieved, but it takes more than 1 h to do so. As described above, the contribution to the photoexcitation from the W-halogen

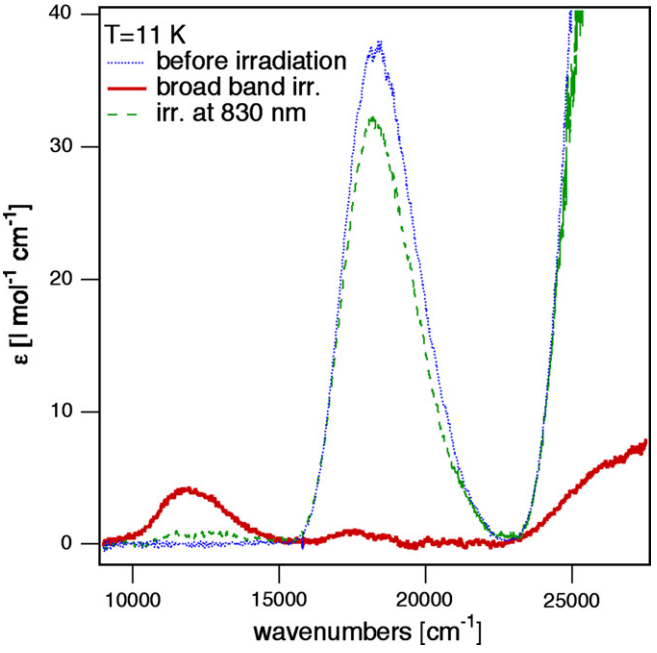

Fig. 3. Single crystal absorption spectra of $[Fe(bbtr)_3](ClO_4)_2$ at 10 K before (. . .) and after (- - -) broad band irradiation using a Xenon arc lamp, followed by irradiation at 830 nm using a red laser diode (—).

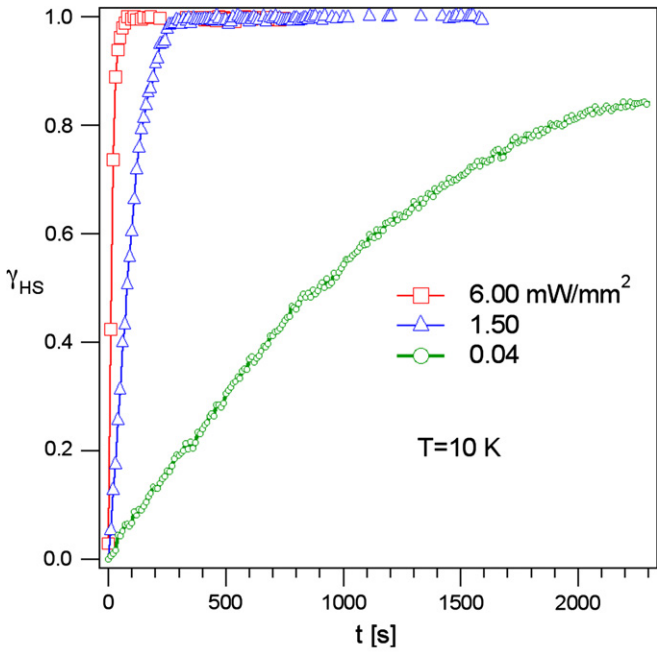

Fig. 4. Photoexcitation curves for the LS → HS transformation of $[Fe(bbtr)_3](ClO_4)_2$ at 10 K during irradiation with different intensities of the 488 nm line of an Ar–Kr cw laser.

lamp is negligible. At 488 nm the optical density of the thin crystal used was <0.2 mm, thus no significant concentration gradients were introduced by the irradiation. No significant incubation time was observed, indeed, the photoexcitation curves are close to single exponential and indicate a quantum efficiency of close to unity, in line with previously reported values [6,35].

Below 50 K the relaxation of the light-induced HS state is too slow to be measured; only above this temperature can it be followed within a reasonable time. Fig. 5 shows absorption spectra during the HS → LS relaxation recorded at 52 K following the quantitative light-induced population of the HS state. In comparison to the thermal spin transition, the baseline shift accompanying the relaxation after photoexcitation is much smaller, indicating that during the relaxation no additional crystal defects are created.

Fig. 6 shows HS → LS relaxation curves plotted as the HS fraction, γ_{HS}, versus time at different temperatures following the quantitative population of the HS state at 10 K and quickly warming to the target temperature. As observed for a number of related compounds, the relaxation curves are sigmoidal, confirming the cooperative character of the spin transition in the compound under investigation. The total relaxation time is more then 7 h at 50 K, it decreases with increasing temperature to 4 h at 55 K and to about 5 min at 65 K. The relaxation curves are reasonably well described by the mean-field equation for cooperative effects, which relates the relaxation rate constant, k_{HL}, to the LS fraction in an auto-accelerating fashion [6]

$$k_{HL}(T, \gamma_{LS}) = (T, \gamma_{LS} = 0) \cdot e^{\alpha(T)\gamma_{LS}} \quad (1)$$

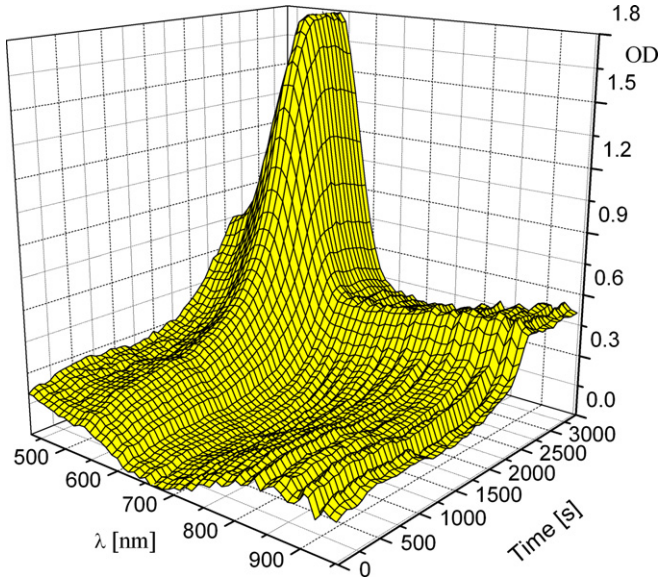

Fig. 5. Single crystal absorption spectra during HS → LS relaxation of $[Fe(bbtr)_3](ClO_4)_2$ following LIESST at 52 K.

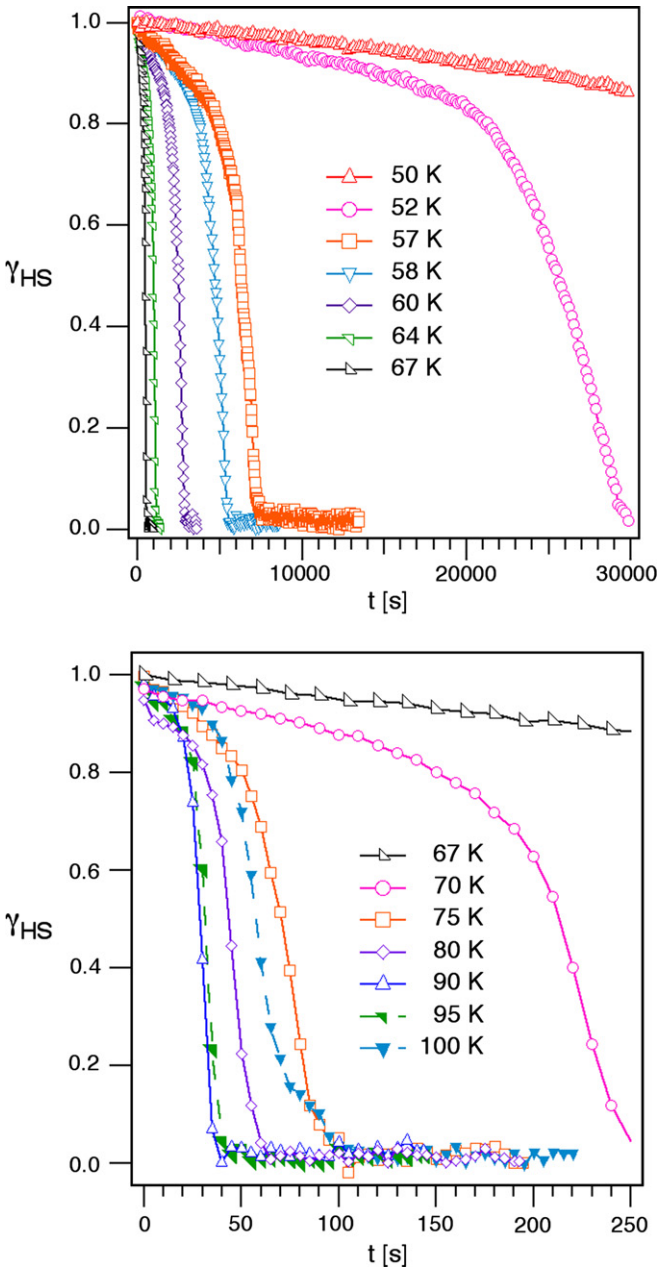

Fig. 6. HS → LS relaxation curves of $[Fe(bbtr)_3](ClO_4)_2$ following LIESST at various temperatures, derived from optical spectra as shown in Fig. 5 for $T = 52$ K.

with α the acceleration factor. Based on the mean-field model k_{HL} (T, $\gamma_{LS} = 0$) should follow an Arrhenius like behaviour above 50 K and α should decrease as $1/T$. However, best fits using Eq. (1) do show systematic deviations from the experimental curves, the acceleration factor $\alpha \approx 6.5$ is almost temperature independent over the whole temperature range, and at temperatures above 70 K the relaxation even though initially still becoming faster with increasing temperature is slower than expected. Finally the HS → LS relaxation even slows down as the thermal transition temperature of 100 K is approached. This can only be explained by quite large short-range interactions leading to fluctuations and the formation of clusters or domains of equal spins [33,36,37].

3.3. The thermal hysteresis

Fig. 7a shows a series of thermal hysteresis loops measured following different protocols. Basically they all are in agreement with the published curve as determined from magnetic susceptibility measurements on a polycrystalline powder [32] showing a hysteresis of approximately 15 K. However, for the single crystals they are much steeper, as previously observed for other spin transition compounds [38]. More importantly, the hysteresis width depends (i) on the temperature sweep rate, indicating that the kinetics of the associated phase transition are very slow indeed, and (ii) on the history of the crystal: when starting from room temperature the apparent transition temperature for the HS → LS transition is lower than when coming from below the thermal transition, heating up to 120 K and then decreasing the temperature again. Thus, at a sweep rate of 0.1 K/min, $T_c^{\downarrow} \approx 97$ K when coming from room temperature and 102 K when coming from 120 K following the first cycle.

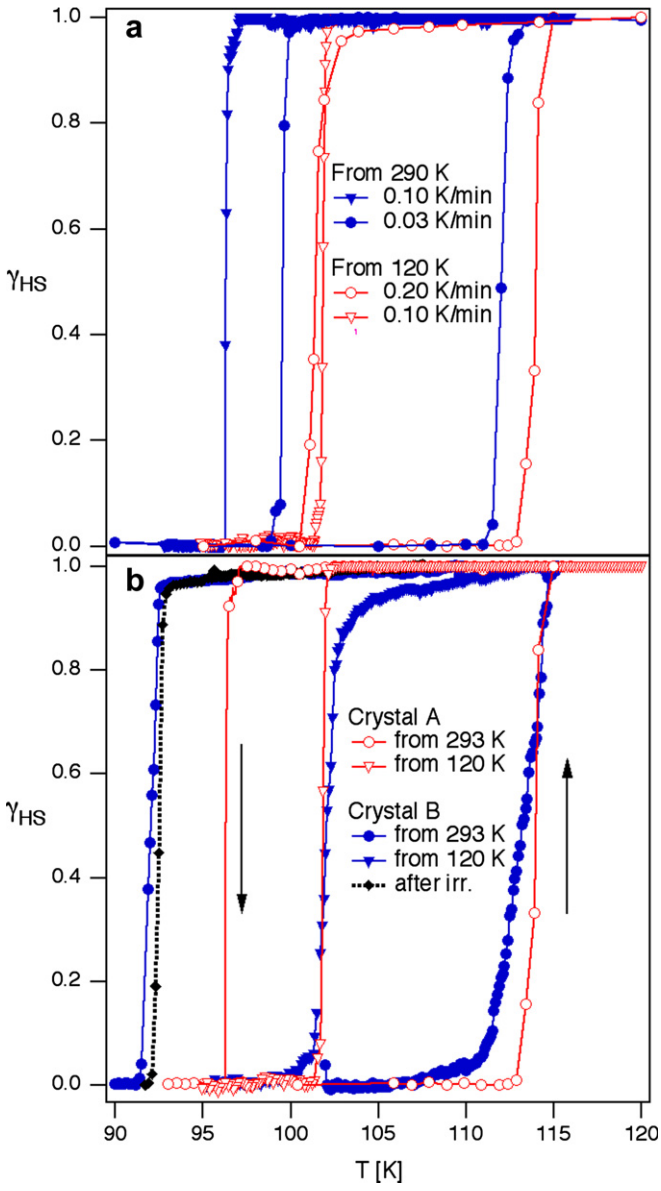

Fig. 7. (a) The thermal spin transition of a single crystal of $[Fe(bbtr)_3](ClO_4)_2$ for different temperature sweep rates and thermal histories of the crystal. (b) The thermal hysteresis of different single crystals of $[Fe(bbtr)_3](ClO_4)_2$ for a temperature sweep rate of 0.1 K/min and different thermal histories, as well as after irradiation.

Fig. 7b shows the hysteresis loops for two different crystals. Whereas $T_c^{\downarrow}$ differs by 6 K when cooling down from the high-temperature phase, it takes on the same value of 102 K for both crystals for the second cycle starting from 120 K. Irrespective of the history of the crystals the LS → HS transition temperature on heating, $T_c^{\uparrow}$, remains the same at 113 K.

In line with this observation goes the fact that the crystallographic structure could be obtained for the HS state at 135 K, but for the LS state at 80 K it failed [32]. All this leads to the conclusion that the thermal spin transition triggers a crystallographic phase transition and that below $T_c^{\downarrow}$ the low-temperature phase has a high degree of disorder. On the first cooling cycle this crystallographic phase transition occurs as a nucleation and growth process and results in the formation of a domain structure [33] depending upon the individual crystal. Upon heating to 120 K, the system returns to the HS state, but retains some memory of this domain structure.

Despite the small temperature sweep rates of the experiment, the apparent transition temperature on cooling depends upon the sweep rate. This indicates that the relaxation is very slow and is governed by the macroscopic nuclear rearrangements of the crystallographic phase transition rather by the intersystem crossing process of the HS → LS relaxation. As shown in Fig. 8, the two different cooling protocols result in very different relaxation curves, measured at constant temperatures just below the respective transition temperatures. As expected for a nucleation and growth process, on cooling from room temperature, the relaxation curves show an initial very slow decrease in the HS fraction for the nucleation process, followed by the typical acceleration of a growth process. For the second cycle, the relaxation curves are almost single exponential. Thus on the second cooling cycle, the preformed domains relax to the LS state in a stochastic process.

Interestingly, the HS → LS relaxation curves also depend upon crystal quality and size. The curves in Fig. 8a were recorded on a comparatively large crystal (diameter ≈0.5 mm) with a non-negligible number of easily discernible defects under a microscope. Fig. 8b shows relaxation curves on cooling from 120 K to the target temperature for a small high-quality crystal (diameter ≈0.3 mm). The relaxation curves are clearly different from the ones in Fig. 8a. The curves at 101 K are quite similar, the relaxation being complete after ~250 s. At somewhat higher temperature, the relaxation curves for the high-quality crystal instead of being comparatively smooth, show distinct steps. This indicates that in the high-quality crystal the number of domains formed during the relaxation process is smaller. The fact that the steps for the curves recorded at different temperatures have roughly the same height is in line with the above mentioned memory effect.

3.4. The temperature quenched state

A key question regards the nature of the temperature quenched HS state: is it similar to the light-induced HS state or are there significant differences. As mentioned above, it has so far not been pos-

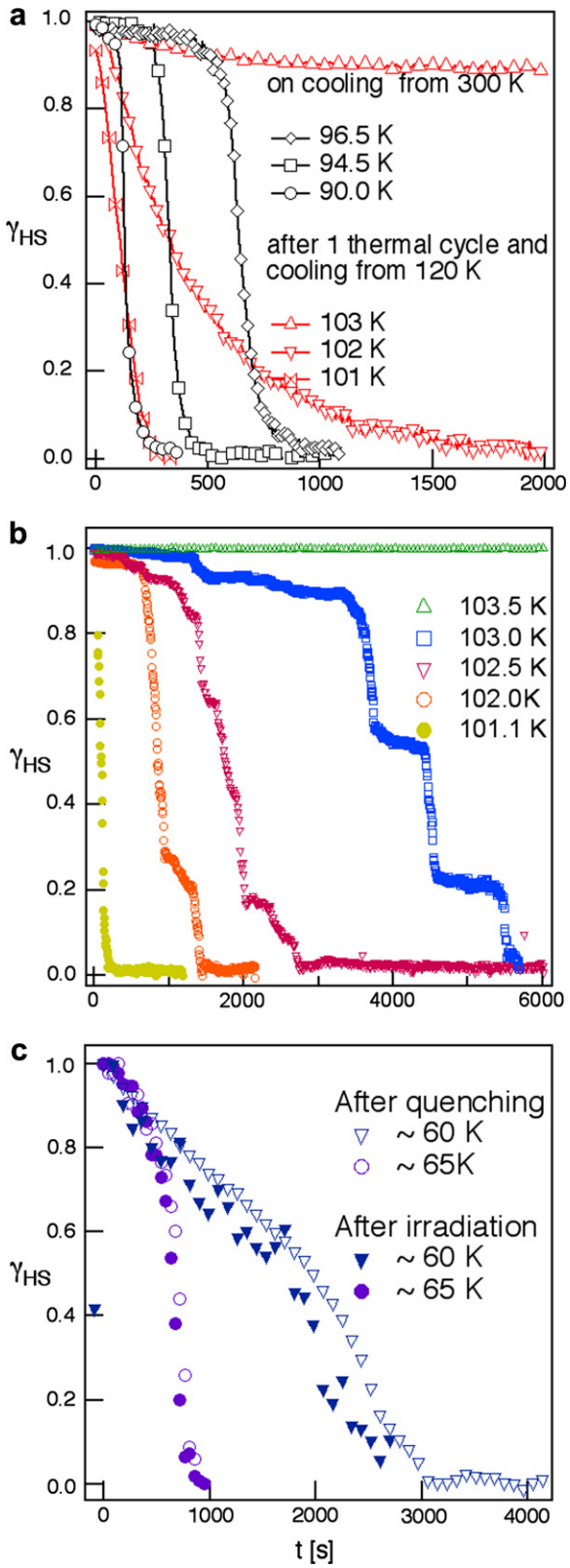

Fig. 8. (a) Relaxation curves for a $[Fe(bbtr)_3](ClO_4)_2$ single crystal at different temperatures when starting the experiment from room temperature (open symbols), and from 120 K on the second cycle (full symbols), adapted from Ref. [33]. (b) HS → LS relaxation curves for a small high-quality crystal around $T^{\downarrow}_c$. (c) HS → LS relaxation curves at 60 and 65 K, after temperature quenching (open symbols) and following irradiation (full symbols).

sible to determine crystal structures below 110 K. A tentative answer can be obtained from the comparison of HS → LS relaxation curves obtained after thermal quenching on the one hand and after irradiation on the other hand. Fig. 8c shows corresponding relaxation curves at 60 and 65 K. The experimental curves at the two temperatures obtained by the two different procedures are identical within experimental error. This indicates that the two metastable HS states are structurally very similar. Provided that the temperature-quenched structure is not too different from the room temperature structure this, in turn, means that the low-temperature irradiation reinstalls some order into the system. This can be correlated to the observation reported in reference [33], that the relaxation curves obtained after irradiation in the neighbourhood of the thermal hysteresis are more in line with the curves of the sample cooled directly from the fully ordered room temperature phase rather than the ones obtained after a thermal hysteresis cycle. This is further supported by the following experiment: a crystal is first quenched from room temperature to 20 K, thus freezing in a HS fraction of 90%. The 10% LS fraction is converted to HS by irradiation and the crystal is warmed to 120 K under constant irradiation such that at all times it is in the HS state. As shown in Fig. 7b, on subsequent slow cooling, the thermal transition curve is identical to the one observed for the cooling cycle starting from room temperature.

4. Conclusions

The two-dimensional polymeric spin-crossover compound $[Fe(bbtr)_3](ClO_4)_2$ shows some remarkable features in its thermal behaviour. The direct bridging of the iron(II) centres in a triangular arrangement results in comparatively strong elastic interactions and hysteresis behaviour. At room temperature, that is, in the HS state, the crystal shows an ordered structure. The spin transition itself triggers a crystallographic phase transition such that at low temperatures, that is, in the LS state, the structure shows a strong degree of disorder. On the first cooling cycle the crystallographic phase transition occurs as a nucleation and growth process and results in the formation of a domain structure with a domain size of the order of the wavelength of light. On subsequent heating to just above $T^{\uparrow}_c$ and renewed cooling the shows a memory effect of the domain structure. The HS → LS relaxation curves following the light-induced population of the HS state at low temperatures show the sigmoidal shape typical for spin-crossover systems with strong cooperative effects. The thermal transition temperature being comparatively low, it is possible to maintain the system in the light-induced HS state all the way up to the transition temperature. Near the transition temperature, the HS → LS relaxation slows down. This is contrary to mean-field theory of cooperative effects and can only be explained by considering strong nearest neighbour interactions leading to fluctuations, and nucleation and growth phenomena. It should be possible to follow the domain formation by temperature dependant optical microscopy. Likewise, pulsed irradiation inside the thermal hysteresis as first demonstrated by Freysz et al. [39], could give further insight.

Acknowledgements

We thank the MAGMANet Network of Excellence of the European Union (Contract: NMP3-CT-2005-515767-2) and the Swiss National Science Foundation for financial support. CE thanks to PNCDI II Romanian CNCSIS Grant "IDEI".

References

[1] P. Gütlich, H.A. Goodwin (Eds.), Spin Crossover in Transition Metal Compounds I–III, Top. Curr. Chem., vol. 233–235, Springer, Heidelberg, 2004.
[2] P. Gütlich, A. Hauser, H. Spiering, Angew. Chem. 106 (1994) 2971.
[3] P. Gütlich, A. Hauser, H. Spiering, Angew. Chem., Int. Ed. 33 (1994) 2024.
[4] P. Gütlich, A.B. Gaspar, Y. Garcia, Y.V. Ksenofontov, C. R. Chim. 10 (2007) 21.

[5] P. Gütlich, V. Ksenofontov, A.B. Gaspar, Coordin. Chem. Rev. 249 (2005) 1811.
[6] A. Hauser, Top. Curr. Chem. 234 (2004) 155.
[7] J.F. Letard, P. Guionneau, L. Goux-Capes, Top. Curr. Chem. 235 (2004) 221.
[8] J.P. Gaudry, L. Capes, P. Langot, S. Marcen, M. Kollmannsberger, O. Lavastre, E. Freysz, J.F. Letard, O. Kahn, Chem. Phys. Lett. 324 (2000) 32.
[9] J. Jeftic, H. Romstedt, A. Hauser, J. Phys. Chem. Solids 57 (1996) 1743.
[10] J. Jeftic, A. Hauser, J. Phys. Chem. B 101 (1997) 10262.
[11] N.O. Moussa, G. Molnar, X. Ducros, A. Zwick, T. Tayagaki, K. Tanaka, A. Bousseksou, Chem. Phys. Lett. 402 (2005) 503.
[12] L.H. Böttger, A.I. Chumakov, C.M. Grunert, P. Gütlich, J. Kusz, H. Paulsen, U. Ponkratz, V. Rusanov, A.X. Trautwein, J.A. Wolny, Chem. Phys. Lett. 429 (2006) 189.
[13] D. Chernyshov, M. Hostettler, K.W. Törnroos, H.-B. Bürgi, Angew. Chem., Int. Ed. 42 (2003) 3825.
[14] J. Kusz, D. Schollmeyer, H. Spiering, P. Gütlich, J. Appl. Crystallogr. 38 (2005) 528.
[15] Y. Miyazaki, T. Nakamoto, S. Ikeuchi, K. Saito, A. Inaba, M. Sorai, T. Tojo, T. Atake, G.S. Matouzenko, S. Zein, S.A. Borshch, J. Phys. Chem. B 111 (2007) 12508.
[16] S. Decurtins, P. Gütlich, C.P. Kohler, H. Spiering, A. Hauser, Chem. Phys. Lett. 139 (1984) 1.
[17] A. Hauser, Coordin. Chem. Rev. 111 (1991) 275.
[18] A. Hauser, J. Jeftic, H. Romstedt, R. Hinek, H. Spiering, Coordin. Chem. Rev. 190–192 (1999) 471.
[19] C.P. Slichter, H.G. Drickamer, J. Chem. Phys. 56 (1972) 2142.
[20] H. Spiering, E. Meissner, H. Köppen, E.W. Müller, P. Gütlich, Chem. Phys. 58 (1982) 65.
[21] J.F. Létard, G. Chastanet, O. Nguyen, S. Marcen, M. Marchievie, P. Guionneau, P. Chasseau, Monatsch. Chem. 134 (2003) 165.
[22] F. Varret, K. Boukheddaden, E. Codjovi, C. Enachescu, J. Linares, Top. Curr. Chem. 234 (2004) 199.
[23] M. Sorai, Y. Maeda, H. Oshio, J. Phys. Chem. Solids 51 (1990) 941.
[24] C. Enachescu, H. Constant-Machado, N. Menendez, E. Codjovi, J. Linares, F. Varret, A. Stancu, Physica B 306 (2001) 155.
[25] C. Enachescu, R. Tanasa, A. Stancu, G. Chastanet, J.F. Letard, J. Linarès, F. Varret, J. Appl. Phys. 99 (2006) 08J504.
[26] N. Huby, L. Guérin, E. Collet, L. Toupet, J.-C. Ameline, H. Cailleau, T. Roisnel, T. Tayagaki, K. Tanaka, Phys. Rev. B 69 (2004) 020101.
[27] G. Molnar, A. Bousseksou, A. Zwick, J.J. McGarvey, Chem. Phys. Lett. 367 (2003) 593.
[28] A. Goujon, B. Gillon, A. Debede, A. Cousson, A. Gukasov, J. Jeftic, G.J. McIntyre, F. Varret, Phys. Rev. B 73 (2006) 104413.
[29] R. Tanasa, C. Enachescu, A. Stancu, E. Codjovi, J. Linares, F. Varret, J. Haasnoot, Phys. Rev. B 71 (2005) 014431.
[30] C. Enachescu, R. Tanasa, A. Stancu, F. Varret, J. Linarès, E. Codjovi, Phys. Rev. B 72 (2005) 054413.
[31] R. Tanasa, C. Enachescu, A. Stancu, F. Varret, J. Linares, E. Codjovi, Polyhedron 26 (2007) 1820.
[32] R. Bronisz, Inorg. Chem. 44 (2005) 4463.
[33] I. Krivokapic, C. Enachescu, R. Bronisz, A. Hauser, Chem. Phys. Lett. 455 (2008) 192.
[34] A. Hauser, P. Gütlich, H. Spiering, Inorg. Chem. 25 (1986) 4245.
[35] C. Enachescu, U. Oetliker, A. Hauser, J. Phys. Chem. B 37 (2002) 9540.
[36] K. Boukheddaden, J. Linares, H. Spiering, F. Varret, Eur. Phys. J. B 15 (2000) 317.
[37] F. Varret, K. Boukheddaden, C. Chong, A. Goujon, B. Gillon, J. Jeftic, A. Hauser, Europhys. Lett. 77 (2007) 30007.
[38] V. Niel, A.L. Thompson, A.E. Goeta, C. Enachescu, A. Hauser, A. Galet, M.C. Munoz, J.A. Real, Chem. Eur. J. 11 (2005) 2047.
[39] E. Freysz, S. Montant, S. Létard, J.F. Létard, Chem. Phys. Lett. 394 (2004) 318.